Integrative modeling of caprock integrity in the context of CO2 storage: evolution of transport and geochemical properties and impact on performance and safety assessment

Olivier Bildstein, Christophe Kervévan, Vincent Lagneau, Philippe Delaplace, Anthony Crédoz, Pascal Audigane, Erwan Perfetti, Nicolas Jacquemet, Michel Jullien

Integrative modeling of caprock integrity in the context of CO_2 storage: evolution of transport and geochemical properties and impact on performance and safety assessment

Bildstein O.[1], Kervévan C.[2], Lagneau V.[3], Delaplace P.[4], Crédoz A.[1], Audigane P.[2], Perfetti E.[4], Jullien M.[1]

[1]CEA, DEN, DTN, Cadarache, 13108 Saint Paul lez Durance, France
[2]BRGM, Service Eau, 45060 Orléans Cedex 2, France
[3]Mines ParisTech, Centre de Géosciences, 77305 Fontainebleau Cedex, France
[4]IFP, Division Ingénierie de Réservoir, 92852 Rueil-Malmaison, France

1. ABSTRACT

The objective of the “Géocarbone-Intégrité” project (2005-2008) was to develop a methodology to assess the integrity of the caprock involved in the geological storage of CO_2. A specific work package of the project (WP5) was dedicated to the integration of (1) the phenomenology describing the evolution of the storage system with a focus on the mechanisms occurring in the caprock and at the interface with the caprock, and (2) the data obtained from the investigation of petrographical, geomechanical, and geochemical properties, before and after reaction with CO_2-rich solutions, performed in the other work packages (WP1 to WP4). This knowledge was introduced in numerical models and specific safety scenarios were defined in order to assess the performance of the CO_2 storage system.

The results of the modeling show that the injection of CO_2 can potentially have a significant effect on the caprock by changing the porosity due to the dissolution and precipitation of minerals, but that the impact is limited to a zone from several decimeters to several meters of the caprock close to the interface with the reservoir depending on whether the supercritical carbon dioxide (SC-CO_2) plume enters into the caprock and if fractures are present at this location.

The methodology used in this project can be applied to a pilot site for the injection of CO_2 in the Paris Basin. A key aspect of the safety of such a facility will be to look at the coupling of geochemical alteration and the evolution of geomechanical properties in the short and medium terms (several hundreds of years). The challenge for the future will be to structure and apply the safety assessment methodology with an operational finality, in order to support the robustness of the transition step to CGS projects at the industrial scale.

2. RESUME

Le Volet 5 du projet « Géocarbone-Intégrité » visait à intégrer l'ensemble des mécanismes étudiés dans les quatre premiers volets du projet pour une évaluation de performance des couvertures et une étude de sûreté afin de s'assurer de leur préservation et de leur intégrité sur le long terme (de l'ordre du millénaire). L’objectif est d’une part d’aboutir à la construction d’un modèle phénoménologique multi-échelle global, puis à un modèle numérique décrivant le confinement du CO_2 par les couvertures et, d’autre part, de déterminer les performances du confinement en identifiant les processus clefs et les paramètres les plus influents.

Une première partie du programme a consisté en une intégration spatiale de l’ensemble des données phénoménologiques et structurales disponibles à la suite des travaux réalisés dans les différents volets (WP1 à WP4) et à la définition des scénarios types d’évolution du site de stockage (niveaux réservoirs et encaissants). Ce travail a permis de définir les cas tests à

prendre en compte et de réaliser les calculs de performance par rapport aux scénarios d'injection et par rapport aux hétérogénéités majeures identifiées dans les niveaux de confinement (notamment les fractures).

Les résultats montrent que l'injection de CO_2 peut avoir un effet significatif, en altérant la porosité par dissolution et précipitation de minéraux, mais que l'impact est limité dans l'espace, de quelques décimètres à quelques mètres de l'interface réservoir-couverture, selon que la bulle de CO_2 supercritique pénètre ou non dans la couverture et selon la présence ou l'absence de fractures.

La prise en compte des résultats issus de l'analyse de sensibilité et l'analyse des incertitudes permettra de conduire des calculs de sûreté plus précis. Appliqués au futur site d'injection, ces calculs permettront d'évaluer la pérennité des propriétés de confinement des couvertures et de valider la qualité de confinement du site de stockage de CO_2. Il conviendra notamment d'évaluer l'impact du couplage entre les phénomènes géochimiques et géomécaniques sur le court et moyen terme (de l'ordre de la centaine d'année). Le défi pour l'avenir est de structurer et d'appliquer la méthodologie de l'analyse de sûreté, en mettant en avant la finalité opérationnelle, de manière à assurer la robustesse de la transition vers les projets de CGS à l'échelle industrielle.

3. INTRODUCTION

The storage of CO_2 in deep saline aquifers and depleted oil and gas reservoirs for periods of time of ~1,000-10,000 years is considered in order to mitigate its release in the atmosphere and avoid the consequences of the additional greenhouse effect on climate change (IPCC, 2005). The feasibility of such an industrial process and the safety on the long term has to be demonstrated and relies mainly on the confinement properties of the caprock. In general, the knowledge of the structure, the properties and the reactivity of the caprock is poor because, usually, the reservoir is the main object of interest for oil and gas production.

The objective of the "Geocarbone-Intégrité" project (2005-2008) was therefore to develop a methodology and to design a tool to assess the integrity of the caprock involved in the geological storage of CO_2. A specific work package of the project (WP5) was dedicated to the integration of (1) the phenomenology describing the evolution of the storage system with a focus on the mechanisms occurring in the caprock and at the interface with the caprock, and (2) the data obtained from the investigation of petrographical, geomechanical, and geochemical properties, before and after reaction with CO_2-rich solutions, performed in the other work packages (WP1 to WP4) (see Fleury et al., *this issue*, for a detailed description of the project). The ultimate goal is to construct a conceptual and numerical model at the site scale to predict the evolution of the storage on the long term and to ensure the persistence of the caprock integrity. This model is developed in the perspective of the assessment of the performance and safety of the future injection pilot site in the Paris Basin planned to be commissioned in 2010.

A review of the existing literature on CO_2 storage modeling reveals that most of the effort made by the scientific community are devoted to the study of injectivity properties and mineral trapping capability in reservoirs (see review by Gaus et al., 2008). The studies on caprock integrity are still relatively rare, and only recently some insights on caprock mineralogical alteration patterns induced by CO_2 migration have been gained by means of reactive transport modeling techniques (Johnson et al., 2004, 2005; Gauss et al., 2005; Xu et al., 2005; Gherardi et al. 2007). This study is focused on the numerical prediction of the long term variations of the mineralogical and hydraulic properties of the caprock in the French pilot site for CO_2 geological storage, in the Paris Basin.

4. PHENOMENOLOGY OF THE STORAGE

4.1. Physicochemical processes at the interface with the caprock

The phenomenology of the storage is described in detail in a special report of the Intergovernmental Panel on Climate Change dedicated to the capture and storage of CO_2 (IPCC, 2005). The injected CO_2 is usually at supercritical conditions (SC-CO_2) in the typical reservoir pressure and temperature conditions (63°C and 145 bar in the case of the Saint Martin-de-Bossenay field - Paris basin, France). Under these conditions, the fluid properties of SC-CO_2 are similar to both a liquid phase (density around 0.6) and a gas phase (low viscosity; e.g. Mathias et al. 2009). Also, CO_2 is very soluble in water: about 1 mol/l (e.g., Duan and Sun, 2003). Its migration in porous media (reservoirs and caprocks) containing water involves capillary effects.

Since SC-CO_2 is less dense than water, it will rise in the reservoir. A fraction of this CO_2 will be trapped in the porosity (capillary trapping) and the rest will reach the structural trap (or stratigraphical trap) constituted by the caprock, which is expected to prevent the CO_2 from rising any further and eventually reaching the atmosphere. This is due to the properties of the caprock which is usually a clay-rich material, saturated with water and characterized by a very low permeability and a high gas entry pressure. The caprock will therefore be in physical contact with the SC-CO_2 plume during most of the storage lifetime.

If the overpressure of SC-CO_2 is lower than the capillary entry pressure, the SC-CO_2 will remain confined in the reservoir. However, dissolved CO_2 will still be able to diffuse into the caprock. This is a slow transport process but the dissolution of CO_2 can strongly affect the composition of the formation water, in particular, by lowering the local pH. This change can potentially damage the caprock by destabilizing the chemical equilibrium with the primary mineral phases and triggering the dissolution of some of them and the precipitation of secondary phases.

If the overpressure at the interface between the reservoir and the caprock overcomes the entry pressure, the SC-CO_2 will penetrate into the caprock, due to the pressure gradient and the buoyancy forces, and will displace the caprock water. If the pressure further builds up, the plume can potentially force its way, in mechanical terms, into the caprock through dilatancy driven flow or induced fracturing.

Importantly, any heterogeneity in the caprock, such as small cracks or fractures, will facilitate the migration of SC-CO_2 into the caprock. The behavior of these preferential pathways and the reactivity with the CO_2-rich fluids is critical for the understanding of the evolution of the confinement properties of the caprock. To this regard, the dissolution of the mineral phase constituting the cement of the rock (e.g. carbonates) can potentially open or close the porosity and affect the permeability of the matrix as well as of the cracks and fractures. The same effect can be obtained by altering potentially expansive primary clay minerals and forming secondary non-swelling ones (e.g. through the illitization process; Crédoz *et al.*, 2009).

A last potentially important migration pathway for CO_2, which was not investigated in this work, is the possibility of having defective abandoned wells present in the zone influenced by the injection.

4.2. Scenarios for the evolution of the storage

The following scenarios have been considered to predict the fate of SC-CO_2 at the interface between reservoir and caprock (Figure 1):

1. The SC-CO_2 overpressure at the top of the reservoir is **lower than the capillary entry pressure in the caprock**. As a consequence, the SC-CO_2 cannot penetrate into the caprock but dissolved CO_2 and acidified formation water can penetrate into the caprock by diffusion, triggering geochemical alteration. This is the ***reference case scenario*** for the safety assessment (section 5.2.1, *case 1a*, *case 1b*, and *case 1c*).
2. The SC-CO_2 does not directly enter into the rock matrix but penetrates the caprock through a network of connected fractures. This is the ***"fracture network" scenario*** which is considered as probable and constitutes a first altered scenario for the safety assessment. Only a dissolved CO_2 is considered in this fracture scenario (section 5.2.2, *case 2*).
3. The SC-CO_2 overpressure at the reservoir top is **higher than the capillary entry pressure in the caprock**. In this case, the SC-CO_2 enters into the caprock by forced drainage. This is the ***multiphase scenario*** where the SC-CO_2 migration is controlled by the effective caprock permeability. This scenario is considered as highly probable in the injection phase (due to significant overpressure) and constitutes a second altered scenario for the safety assessment (section 5.3, *case 3*).

The chosen scenarios mainly focus on the geochemical effects induced by the advancement of both a CO_2-rich aqueous phase and a free SC-CO_2 gas plume through the caprock. A fractured caprock scenario is also simulated but the focus is concentrated on geochemical reactions with the filling material (calcite). In this work, worst case scenarios based on "hydrodynamic" leaking of CO_2, e.g. through open fractures, are not investigated and therefore the results presented here does not constitute a full safety assessment exercise.

The effect of gas-rock interactions has not been considered in our calculations because most of the reactivity is expected to occur at the interface between rock and aqueous phase. This is supported by the fact that high residual water contents (liquid saturation, S_L, always greater than about 0.6) have been calculated even for the case of most significant penetration of SC-CO_2 into the caprock.

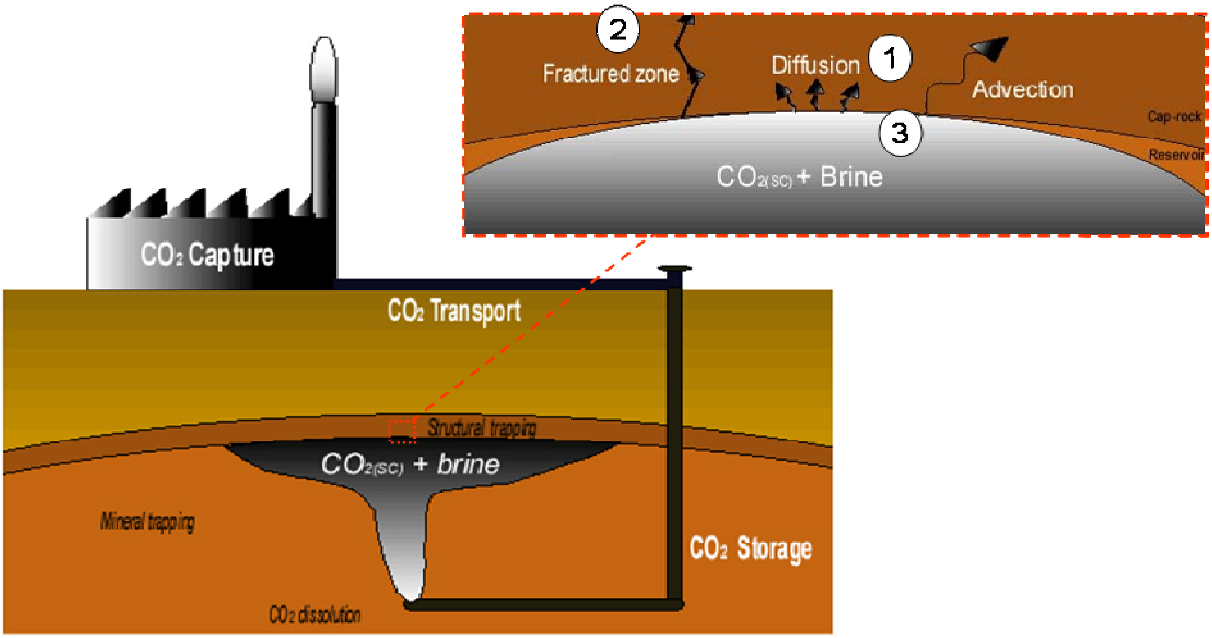

Figure 1. Scenarios for the evolution of the reservoir/caprock system during CO_2 injection.

5. ASSESSMENT OF CAPROCK INTEGRITY PERSISTENCE WITH TIME

The impact of geochemical alteration of the caprock, in terms of confinement properties, on transport properties such as permeability depends primarily on the initial value of these parameters and on the net volume balance of mineral reactions, i.e. dissolution and precipitation (Bemer and Lombard, 2009).

The geochemical reactivity of the caprock and its constitutive minerals has been investigated in WP4 of the “Géocarbone-Integrité” project which aimed at determining the reaction pathways for SC-CO_2/water/rock interactions and also kinetic parameters for carbonate and clay mineral transformations (Kohler and Parra, 2007; Crédoz *et al.*, 2009; Hubert, 2009).

These parameters have to be integrated into large scale modeling in order to calculate the evolution of the storage system as a result of the CO_2 perturbation. A major challenge of this type of modeling is to extrapolate the behavior of the system from the lab scale to the field scale, including:

- time: 1 year for experiments vs. 10,000 years for geological storage,
- solid/solution ratio: around 50 g/L in experiments vs. about 50 kg/L in depth,
- texture: fine crushed rock (0.1 mm particles) vs. bulk rock,
- temperature: 80-150°C in the experiments vs. 65°C in Saint Martin-de-Bossenay (Paris Basin, France).

In the laboratory, the conditions are chosen so that the reactivity of the samples is enhanced in order to limit the duration of the experiments. For the large scale calculations, it is crucial to set these parameters to realistic values but the effect of the texture is difficult to determine except through values of the reactive surface area. Petrophysical and geochemical parameters are given for the different scenarios considered in Table 1 which are used for 1D and 2D calculations with a simplified caprock geometry (15% porosity, 1 to 10 meters thick).

5.1. Modeling approach

At the beginning of the project, the collaborative work between different modeling teams was organized much in the same way as the IPCC modeling of climate (IPCC, 2007), i.e. defining a set of common guidelines and parameters for the modeling (Table 1) but also giving some degree of liberty concerning the way to carry out the calculations, in particular:

- the choice of the numerical tool,
- the capillary and permeability properties,
- the list of secondary minerals allowed to precipitate, and to some extent of primary minerals as well,
- the values for the mineral kinetic constants for precipitation and dissolution and the reactive surface area,
- the feedback between mineral dissolution/precipitation and the transport parameters (diffusion coefficient, permeability, capillary curve, …)

In this way, the modeling exercise should not be considered as a benchmarking of different modeling tools but rather as an investigation of the dominant processes and the most influential parameters giving an envelope of behaviors for the storage system. Only one representative set of results is shown for a specific scenario if all the modeling teams involved in the calculations reached the same conclusions. If the conclusion is significantly different, a comparison and analysis of the results is presented.

Guidelines for the modeling scenarios

A first series of calculations in scenarios where the porous media are saturated (Table 1: cases 1a to 1c and case 2, respectively corresponding to scenarios 1 and 2) were performed with reactive transport tools available in the different modeling teams: Crunch (Steefel, 2001), Hytec (van der Lee et al., 2003), PhreeqC (Parkhurst and Appelo, 1999), PHAST (Parkhurst et al. 2004). The thermodynamic database used for the calculations is derived from EQ3/6 code (Wolery, 1992), and the kinetic data for the dissolution (and to a lesser degree for the precipitation) of mineral phases were taken from the review by Palandri and Kharaka (2004).
A second series of calculations using the same scenarios involved multiphase flow and reactive transport in porous media (Table 1: case 3 corresponding to scenario 3) and were performed with TOUGHREACT (Xu and Pruess, 2001) and COORES™ (e.g. Le Gallo et al. 2007).

Reference case		**Sensitivity analysis**
Duration = 10000 years - Temperature = 80℃		
Caprock initial composition	based on Charmotte/Saint Martin-de-Bossenay (Paris basin)	
Water initial composition	in equilibrium with caprock mineralogy (pH = 6.5)	
Boundary condition (constant concentration)	(1a) acidified water starting from Dogger formation $CO_2(aq)$ = 1.1 molal in equilibrium with pCO_2 = 150 bar (pH = 4.7) (1b) initial composition acidified with pCO_2 = 150 bar and buffered with carbonates (pH = 4.6) (1c) initial composition acidified with pCO_2 = 150 bar (pH = 3.4)	(1a) water from Dogger formation (pH = 6.2) (1b) initial composition acidified with pCO_2 = 150 bar (pH = 3.4)
1) 1D Diffusive/convection case (1a, 1b, 1c)		

Porosity	15%	(1a) 5%
Effective diffusion coefficient	10^{-11} m^2/s	(1a) 10^{-10} m^2/s
Permeability Flow rate	(1c) K = 1.6 10^{-18} m^2 10x diffusive flux	
2) 2D system with discrete fracture (case 2)		
Mineralogy and water composition	based on case 1c	
Fracture filled with calcite	porosity 40%	
Fracture permeability	10,000 x higher than in reservoir (case 1c)	
3) 1D multiphase case (case 3)		
Mineralogy and water composition	based on single-phase case 1a	
Boundary condition	constant pressure	
Relative permeability	Van Genuchten model (see Eq. 1 and 2) K = 10^{-18} m^2	
Capillary pressure	Van Genuchten model (see Eq. 3)	
Effective diffusion coefficient	10^{-11} m^2/s	

Table 1. Modeling parameters for the reference case simulation and sensitivity analyses.

Note that for the boundary conditions, the chemical composition of reservoir pore waters remain fixed during the simulation. For the cases with acidified waters, it means that the pH in the reservoir is controlled by the CO2-plume during 10,000 years, even though control should be taken over by the reservoir water composition again at some point after the end of the CO_2 injection. It is however considered here as a conservative assumption for the performance and safety of the storage.

5.2. Saturated caprock: geochemical interactions with dissolved CO_2

In these scenarios, the SC-CO_2 plume is trapped in the reservoir and the acidic perturbation migrates by diffusion of dissolved species only.

5.2.1. Homogeneous caprock, diffusive/advective case

In these calculations, the diffusion coefficient is set initially to 10^{-11} m^2/s, which is the mean value measured in the argillites from Bure (Talandier et al., 2006) and considered as analogues to the clay series in the caprock investigated in the framework of this project. More details about diffusion coefficients can be found in Fleury et al. (2009) and Berne et al. (2009). Some sensitivity calculations are also shown which investigate the influence of this parameter.

Case 1a: pure diffusion, specific water compositions for the reservoir and caprock

In this case, the caprock is initially homogeneous in composition (mineralogy and pore water) and in transport properties (no cracks or fractures or other preferential pathways). Preliminary batch calculations were conducted in order to determine possible secondary mineral phases that potentially precipitate in this context. Some simplifications were made in the calculations in order to avoid dealing with complex solid-solutions: clay minerals are represented only by pure end-members (it concerns especially the interstratified illite-smectite minerals), mixed carbonates such as ankerite are considered with a constant composition (Table 3). In this series of simulations, the acidified water ($pCO_2 = 150$ bar) used as the boundary condition at the contact with the caprock is equilibrated with the mineral assemblage of the reservoir. Under this hypothesis, the water can be considered as less aggressive with respect to the caprock minerals than in the configuration where the water is only acidified by CO_2 (*case 1b*). The water compositions considered here, based upon data from Azaroual et al. (1997), are detailed in Table 2.

A 1D geometry was considered within the caprock assuming an initial equilibrium between the water (Table 2, 3rd column) and the mineral phases constituting the caprock (Table 3). The base of the modeled domain was supposed to be permanently in contact with the acidified reservoir water (Table 2, 2nd column) so that dissolved CO_2 is transported by molecular diffusion within the caprock.

We performed several simulations considering various typical initial porosities (15 and 5%) and diffusion coefficient values (10^{-11} and 10^{-10} $m^2.s^{-1}$). The codes PHREEQC and PHAST were used with various meshes (about 100 grid cells, with both uniform and variable grid spacing) and time-stepping in order to increase the robustness of the calculations presented hereafter (Figure 2 and Figure 3).

Reference Dogger reservoir water (80°C)*		**Acidified reservoir water (80°C, pCO_2 = 150 bar)***		**Initial caprock water (80°C)**	
pH	6.24	**pH**	4.75	**pH**	6.54
Species	**Molality**	**Species**	**Molality**	**Species**	**Molality**
Al	$5.622\ 10^{-8}$	Al	$1.251\ 10^{-7}$	Al	$1.531\ 10^{-7}$
C	$4.895\ 10^{-3}$	C	1.141	C	$2.180\ 10^{-3}$
Ca	$1.612\ 10^{-2}$	Ca	$3.204\ 10^{-2}$	Ca	$1.528\ 10^{-2}$
Cl	$3.014\ 10^{-1}$	Cl	$3.015\ 10^{-1}$	Cl	$2.601\ 10^{-1}$
Fe	$2.137\ 10^{-7}$	Fe	$1.751\ 10^{-6}$	Fe	$1.534\ 10^{-5}$
K	$2.374\ 10^{-3}$	K	$2.375\ 10^{-3}$	K	$1.190\ 10^{-2}$
Mg	$1.282\ 10^{-2}$	Mg	$2.424\ 10^{-2}$	Mg	$8.937\ 10^{-4}$
Na	$2.594\ 10^{-1}$	Na	$2.595\ 10^{-1}$	Na	$2.543\ 10^{-1}$
S	$7.642\ 10^{-3}$	S	$7.649\ 10^{-3}$	S	$1.841\ 10^{-2}$
Si	$8.994\ 10^{-4}$	Si	$8.833\ 10^{-4}$	Si	$5.371\ 10^{-4}$

(*) equilibrated with the assumed reservoir mineralogy (calcite, dolomite-dis, chalcedony, illite, pyrite)

Table 2. Water compositions considered in the simulations.

Mineral phase	**Initial weight %**	**log(K) at 80°C**	**reaction**	**SI(1)**	**SI(2)**	**SI(3)**
Calcite	50	1.05	Calcite + $H^+ = Ca^{++} + HCO_3^-$	0	0	0
Ankerite	5	12.14	Ankerite + $4H^+ = Ca^{++} + 0.3Mg^{++} + 0.7Fe^{++} + 2H_2O + 2CO_{2(aq)}$	-0.99	-0.99	0
Montmorillonite-Na	25	-0.65	Mont-Na + $6H^+ = 0.33\ Mg^{++} + 0.33\ Na^+ + 1.67Al^{+++} + 4H_2O + 4SiO_{2(aq)}$	0.77	0.52	0
Kaolinite	3	2.38	Kaolinite + $6H^+ = 2Al^{+++} + 2SiO_{2(aq)} + 5H_2O$	0.13	1.49	0
Illite	2	3.80	Illite + $8H^+ = 0.25Mg^{++} + 0.6K^+ + 2.3Al^{+++} + 3.5SiO_{2(aq)} + 5H_2O$	0	0	0
Quartz	10	-3.24	Quartz = $SiO_{2(aq)}$	0.23	0.23	0
Anhydrite	3	-5.05	Anhydrite = $Ca^{++} + SO_4^{--}$	-0.47	-0.34	0
Pyrite	2	-21.91	Pyrite + $H_2O = 0.25H^+ + 0.25SO_4^{--} + Fe^{++} + 1.75HS^-$	0	0	0
Goethite	-	-1.13	Goethite + $3H^+ = Fe^{+++} + 2H_2O$	-2.65	-5.20	6e-4
Chalcedony	-	-3.02	Chalcedony = $SiO_{2(aq)}$	0	0	-0.23
Disordered-Dolomite	-	1.92	Dolom-dis + $2H^+ = Ca^{++} + Mg^{++} + 2HCO_3^-$	0	0	-1.24
Siderite	-	-1.17	Siderite + $H^+ = Fe^{++} + HCO_3^-$	-2.78	-2.78	-0.84

Table 3. Initial mineral composition of the caprock (inspired from the Charmotte field) and secondary phases (*in italics*) taken into account in the model. Equilibrium constants at 80°C and reactions are given for each mineral. SI(1), SI(2), and SI(3) refer to the initial saturation indexes of the mineral phases in the Dogger, acidified, and caprock waters respectively.

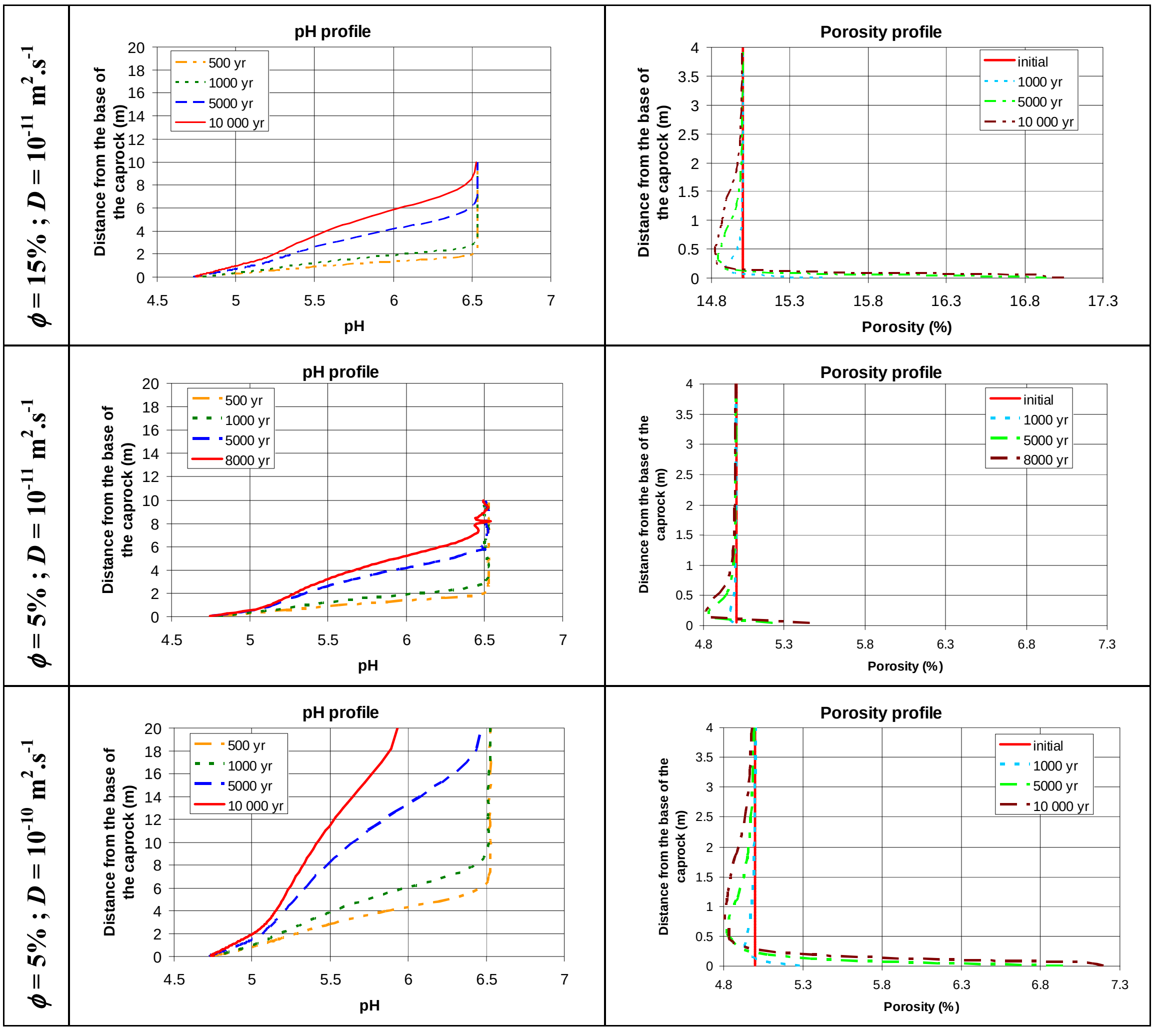

Figure 2. Diffusion of the acidified reservoir water: pH and porosity profiles in the caprock calculated for several porosity (15 and 5%) and diffusion coefficient (10^{-11} and 10^{-10} $m^2.s^{-1}$) values. (Note zoom over 4 m in porosity profiles)

In all cases, similar trends and orders of magnitude for pH and porosity profiles along the first few meters of the caprock are observed after a simulation period up to ten thousands years (Figure 2). As expected, the acidified water penetrates the caprock on a distance increasing with the diffusion coefficient value (see pH profiles). However, the impact on the minerals remains comparable (mainly: dissolution of illite and anhydrite, precipitation of calcite, montmorillonite-Na and kaolinite), showing no significant sensitivity towards initial porosity and diffusion coefficient values, as illustrated by the porosity profiles which integrate the volumetric variations of all the primary and secondary mineral phases considered in the chemical reactions (see Table 3). In all cases, both the amplitude and the extension of the variations observed along the modeled profile remain relatively limited: a first increase in porosity (up to +2.2%) within the first decimeters of the caprock domain is observed, followed by a slight decrease of the porosity value (around -0.2%) in the next 1 to 3 meters.

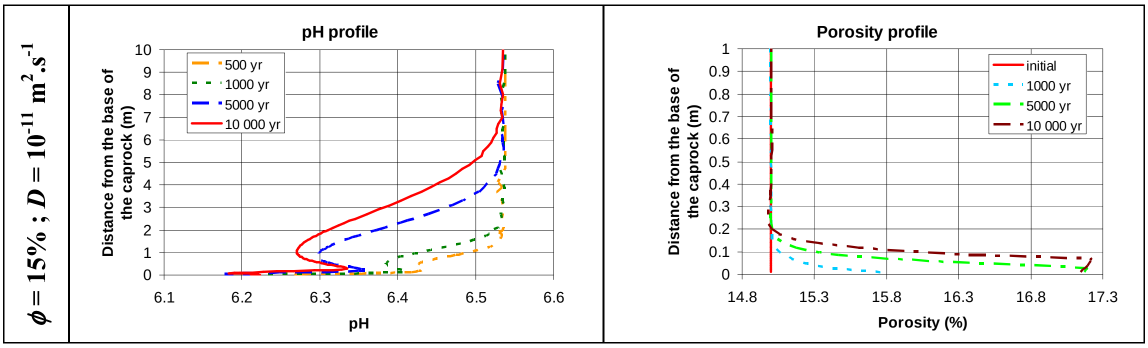

Figure 3. Diffusion of the non-acidified reservoir water: pH and porosity profiles in the caprock calculated for a porosity of 15% and a diffusion coefficient of 10^{-11} $m^2.s^{-1}$.

Note that the water compositions described in Table 2 also show a significant contrast between the initial caprock water and the original reservoir water. Formation water indeed often show differences which are not completely balanced by diffusion at the interface. Interdiffusion processes can potentially induce some transformations in the mineral composition at this location. In order to quantify this effect and discriminate the role of dissolved CO_2, we performed another simulation for the first parameter set ($\phi = 15\%$; $D = 10^{-11}$ $m^2.s^{-1}$) now using columns 1 and 3 in Table 2 as boundary and initial water compositions, respectively. The results obtained are presented in Figure 3. As expected, pH variations along the profile are much smaller in amplitude than in the "acidified water" case (ranging here between 6.2 and 6.5). The behavior of the system, in terms of mineral reactivity, is comparable to the previous simulations with acidified water (*i.e.*, dissolution of illite and anhydrite, precipitation of calcite, montmorillonite-Na and kaolinite) but remains limited to the very first decimeters of the caprock. However, the impact on porosity is significant as shown by the porosity profiles in Figure 3. When compared to the profiles in Figure 2, it can be noticed that the amplitude of the increase in porosity (varying from 15 to 17%) is quite similar. In this case, however, no decrease of the porosity is observed in the first meter of the caprock.

The results obtained in this last simulation give us some new insight into the specific role of the initial water composition and the pH perturbation due to CO_2. The distinct impact of the initial water was also observed in experiments where the caprock from the Paris Basin was reacted with typical reservoir water from the Dogger formation (Crédoz et al., 2009).

Case 1b: pure diffusion, same initial water composition in reservoir and caprock

The mineral composition corresponds to that of the transition zone between the reservoir and the caprock in the Charmotte area (Paris Basin, France) (Table 4). The initial water composition is in equilibrium with the mineral assemblage of the caprock. Two water compositions are considered at the boundary (i.e. at the interface between the caprock and the reservoir). In both case, the water is similar to the previous one, except for the acidification of the water due to the dissolution of CO_2 in the reservoir (Table 5). For the first one, we consider the acidification effect but also some short term buffering capacity of minerals (essentially carbonates and sulfates) which reacted with the CO_2 plume and the solution during the migration of the plume in the reservoir. This case resembles the previous *case 1a* (pH = 4.63). For the second one, we consider that the acidification is maximized (pH = 3.36, in equilibrium with CO_2-SC only) in order to obtain the strongest pH perturbation possible in this system, i.e. testing extremely adverse conditions for safety assessment purposes. This scenario corresponds to a hypothetical case in which the minerals from the reservoir do not buffer the pH (i.e., the residence time of the interstitial water is much shorter than the reaction kinetics characteristic time).

	Volume % (fraction of total rock volume)	Weight % (of solid)
Porosity	*15*	-
Clay fraction		
Illite	11	13
Montmor-Ca	2	3
Kaolinite	9	10
Silt fraction		
Quartz	9	10
Carbonate fraction		
Calcite	41	45
Dolomite	2	3
Siderite	1	2
Accessory minerals		
Pyrite	2	4
Anhydrite/gypsum	4	5
Anatase, other …*	4	5

* considered as inert minerals

Table 4. Simplified composition used for calculations with the transition zone between reservoir and caprock at Charmotte (porosity = 15%).

Charmotte transition zone water composition (80°C)*		**Acidified water (80°C, pCO_2 = 150 bar, fCO_2 = 83 bar)**		**Acidified water equilibrated with carbonates* (80°C)**	
pH	6.20	**pH**	3.36	**pH**	4.63
Species	**Molality**	**Species**	**Molality**	**Species**	**Molality**
Al	$2.18\ 10^{-8}$	Al	$2.18\ 10^{-8}$	Al	$1.21\ 10^{-8}$
C	$2.00\ 10^{-3}$	C	1.00	C	1.02
Ca	$4.22\ 10^{-2}$	Ca	$4.22\ 10^{-2}$	Ca	$5.50\ 10^{-2}$
Cl	$1.92\ 10^{-1}$	Cl	$1.92\ 10^{-1}$	Cl	$1.92\ 10^{-1}$
Fe	$1.22\ 10^{-5}$	Fe	$1.22\ 10^{-5}$	Fe	$9.30\ 10^{-6}$
K	$1.85\ 10^{-2}$	K	$1.85\ 10^{-2}$	K	$1.85\ 10^{-2}$
Mg	$1.12\ 10^{-2}$	Mg	$1.12\ 10^{-2}$	Mg	$1.52\ 10^{-2}$
Na	$8.00\ 10^{-2}$	Na	$8.00\ 10^{-2}$	Na	$8.00\ 10^{-2}$
S	$6.16\ 10^{-3}$	S	$6.16\ 10^{-3}$	S	$5.86\ 10^{-3}$
Si	$6.55\ 10^{-4}$	Si	$6.55\ 10^{-4}$	Si	$2.48\ 10^{-4}$

* *equilibrated with fast reacting minerals assumed to be present in reservoir (calcite, dolomite, anhydrite)*

Table 5. Water compositions considered in the simulations.

The calculations concerning the scenario with the pH 4.6 water entering the caprock shows that the alteration of the caprock is significant with a similar front of pH perturbation compared to *case 1a*, but the porosity change is very limited (Figure 4). The precipitation of anhydrite (+16%), kaolinite (+12%) and quartz (+2%) is responsible for the porosity decrease observed directly at the reservoir-caprock interface (down to 8% porosity in the first centimeter). Illite (-11%), calcite (-6%), and montmorillonite (-2%) dissolution is also observed at this location. Calcite dissolution and anhydrite precipitation occurs only in this first zone, and a very narrow zone where the montmorillonite remains stable explains the modest change in porosity (+1%) over a few centimeters. A third zone where clay minerals (illite and montmorillonite) are destabilized but with precipitation of kaolinite, K-feldspar, and quartz results in a slight decrease of porosity (1 to 2%). The paragenesis is slightly different from *case 1a*, especially concerning the behavior of calcite and anhydrite. In *case 1b*, calcite dissolves and anhydrite precipitates in the sulfate-rich caprock water. These differences arise from slightly different hypotheses concerning the initial water compositions: a complete set of minerals is used in *case 1a* (Table 3) *vs*. "fast reacting" minerals only in *case 1b* (Table 5). In both cases, however, the impact on the porosity profile remains comparable.

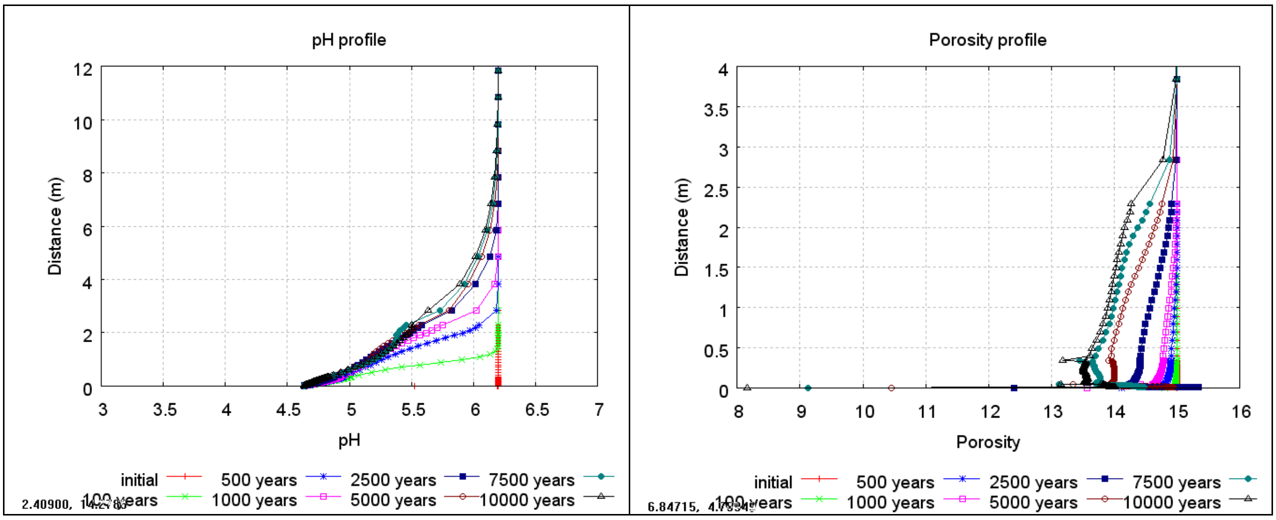

Figure 4. Porosity and pH profiles in the caprock in the case with buffering capacity of the reservoir (pH 4.6). Note the difference of zooming in distance.

The calculations concerning the scenario with the most aggressive water entering the caprock show a significant alteration of the caprock at the interface, in comparison to the previous case, with a concomitant increase in porosity (Figure 5). The dissolution of carbonate (calcite and dolomite) and clay minerals (illite and montmorillonite) is responsible for the increase of porosity from the initial 15% to an average value of 85% in the first centimeters directly at the interface, even though kaolinite, anhydrite, and quartz precipitate at this location. A second front of porosity increase (to almost 60%) reaches 50 centimeters into the caprock and corresponds to the front of dissolution of carbonates only (calcite and dolomite). The same minerals as in the first front area also precipitate in this zone, except for anhydrite which shows a dissolution, up to 15 centimeters, and then a precipitation pattern. Porosity and pH variations are closely correlated in these calculations.

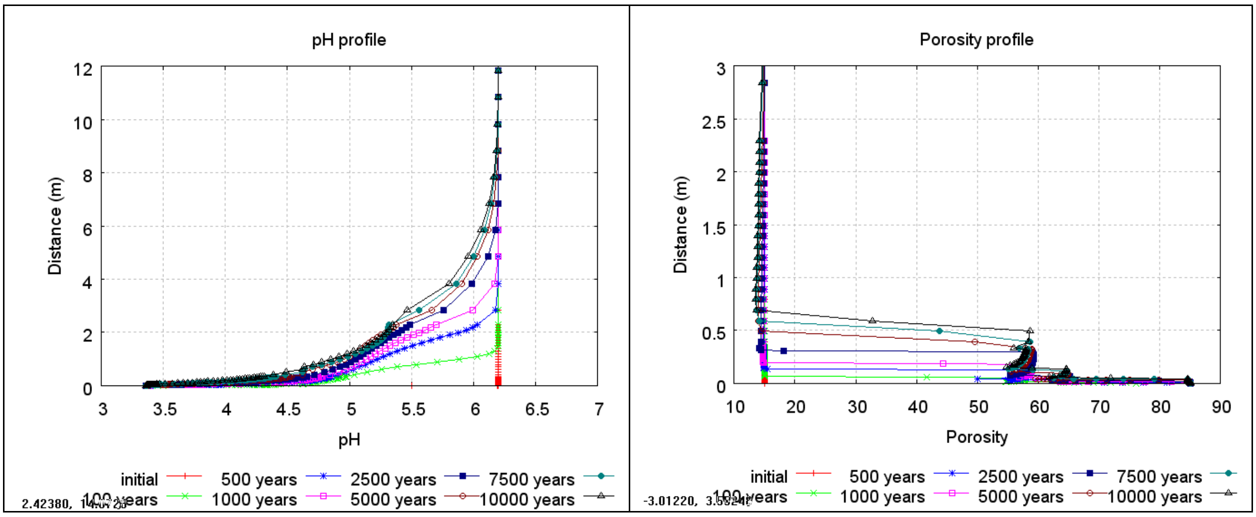

Figure 5. Porosity and pH profiles in the caprock in the case without buffering capacity of the reservoir (pH 3.4). Note the difference of zooming in distance.

The results show that in this diffusive case, the caprock alteration can be significant and the impact on porosity greatly depends on the water composition and, in particular, on the pH of the solution. In the case of aggressive water with low pH, all the primary minerals are strongly destabilized directly at the interface between the reservoir and the caprock. A significant increase of porosity is also further predicted but the extent remains limited to 50 centimeters: this sharp porosity front corresponds to the complete dissolution of carbonate minerals (calcite and dolomite) where the other primary minerals are rather preserved, resulting in a porosity increase of about 45%. In the interval between these two fronts, mineral adjustments occur leading to an overall "Z-shaped" porosity profile: dissolution of illite and montmorillonite; precipitation of kaolinite and quartz.

This scenario represents an extreme case where no minerals in the reservoir act as buffer of the pH perturbation, and exemplify the role of the pH of the water at the interface between the reservoir and the caprock. Note also that the mechanical strains that would accommodate at least part of this porosity increase are not taken into account in these calculations. In the other case, the behavior of the system would tend to a slight decrease of the porosity (1%) affecting 3 meters of the caprock. Consequently, if the SC-CO_2 stays confined in the reservoir, the impact of the acidic perturbation on the overall confinement function of a caprock, with a couple of decimeters thickness, will be very low.

Case 1c: diffusion/slow advection, same initial water composition in reservoir and caprock

A slightly degraded version of the previous diffusive scenario was simulated. This scenario integrates the effect of a small overpressure in the reservoir compared to the overlying aquifers. This overpressure can result from the injection itself or from the regional hydrological conditions. However, the scenario considers that the overpressure remains low enough so as not to enable a capillary breakthrough of the SC-CO_2: as a result, only dissolved CO_2 (along with the chemical background of the reservoir pore water) can migrate advectively into the caprock.

An upwards 5 mm/y flow was simulated; this would correspond to a 1 m/m hydraulic head gradient with 1.6 10^{-18} m^2 permeability, a large upper value for the permeability of a deep argillaceous caprock (e.g. Hildenbrand and Kroos, 2003). The diffusive simulations from *case 1b* (low pH) are reproduced, integrating this slow advection. In particular, the sharp fronts and the overall "Z-shaped" behavior in the porosity profile are predicted, even though they slightly differ in amplitude (maximal increase is 30%). Identical reaction pathways are identified, with reaction fronts progressing slightly faster than in the diffusive case. However, the progression of the fronts remains limited to the close vicinity of the reservoir/caprock interface: Figure 6 shows a migration limited to 0.5 m after 10000 y.

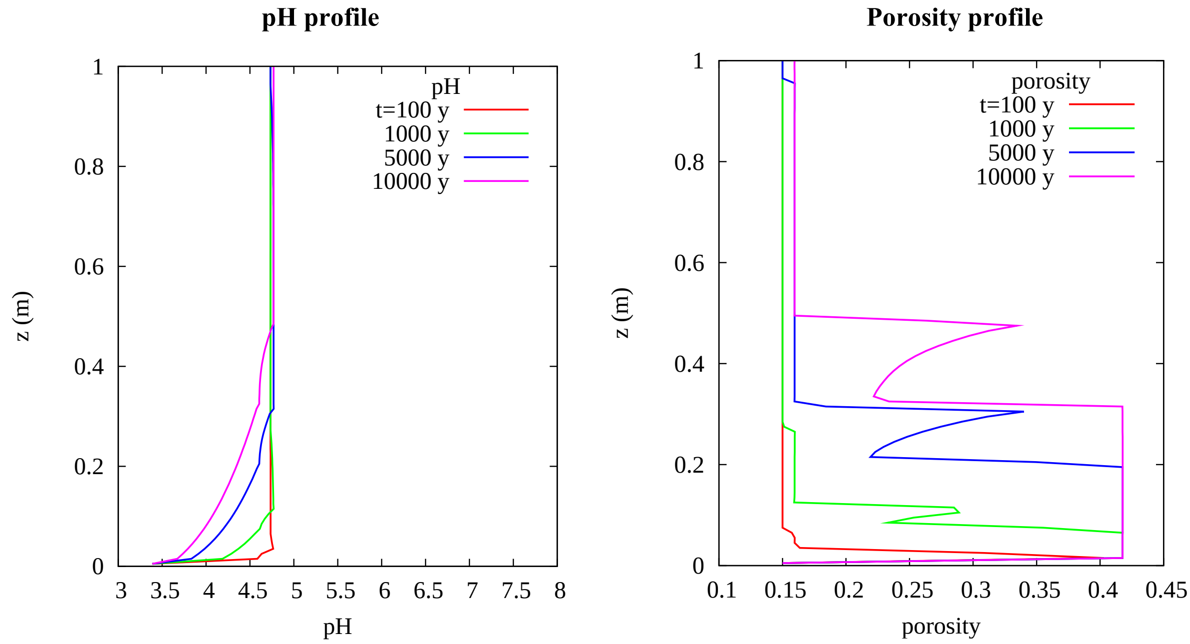

Figure 6. Advection/dispersion of CO2-rich solution into the caprock: pH and porosity profile as a function of time.

The diffusive-advective scenario simulations show that the migration of dissolved CO_2 remains confined to the first few decimeters of the caprock after hundreds of years under normal hydrological assumptions: homogeneous caprock, quasi natural regional hydraulic gradients between the aquifers, no capillary breakthrough.

Conclusion on the diffusive case

As a general conclusion to the calculations in homogeneous diffusive/advective conditions, we can consider that this case allows us to define a useful reference case for a better interpretation of the potential impact of the acidified water diffusion along the caprock. Under the assumptions and the initial and boundary conditions considered here, the impact of the diffusion of dissolved CO_2 in the caprock is very limited in vertical extension (first decimeters to meters after 10,000 yrs). The amplitude depends essentially on the pH of the water in the reservoir at the interface with the caprock (a 45% increase in porosity in the first 50 centimeters in the adverse case of low pH for the reservoir water). In these scenarios, the long term consequences of the CO_2 perturbation on the caprock integrity thus appear to be small, especially in the context carbonate-dominant storage systems.

The same conclusions are reached by other authors in the literature with slightly different reactive pathways and consequences on porosity, due to the differences in the initial mineralogy. In particular, the presence of plagioclase minerals that tend to dissolve, eventually leads to the precipitation of minerals such as dawsonite (Gauss et al., 2005;

Gherardi et al., 2007). The intensity of the reactions and porosity changes (up to 10%, with comparable increasing and decreasing patterns) modeled by these authors are similar to those observed in this work, even though the temperature was lower (~40°C).

5.2.2. Caprock with discrete fracture

Case 2: diffusive/advective transport in discrete fracture

To investigate the effect of local heterogeneities in the caprock, the advective scenario (*case 1c*) was degraded with the presence of a discrete fracture. The simulation was translated into vertical 2D, with an explicit fractured zone: a 5 mm wide half-fracture is created into a homogeneous caprock, on a 10 m high simulation. A 0.1 m/m hydraulic gradient was given, with a 1.6 10^{-18} m^2 permeability in the bulk matrix, and a permeability 10^4 times higher in the fractured zone (corresponding to 5 mm/y upflow rate). The chemistry in the matrix is taken identical to that of the previous reference simulations (*case 1c*); the fractured zone is considered filled up with calcite, with a remaining porosity of 0.4. These conditions constitute upper values for a realistic system, in agreement with the safety assessment rules of the exercise.

The simulation results (Figure 7) show a degradation front in the bulk matrix far from the fracture, in agreement with the previous homogeneous simulations in terms of amplitude. Closer to the fracture, the locally enhanced flow brings more reacting CO_2 vertically into the system, so that the reaction front is accelerated (both vertically and horizontally). Inside the matrix itself, the reaction front is even faster, with a positive feedback of the dissolution of the calcite, which additionally enhances the fluid flow with the increased permeability in the reacted area (increased by a factor 10^3).

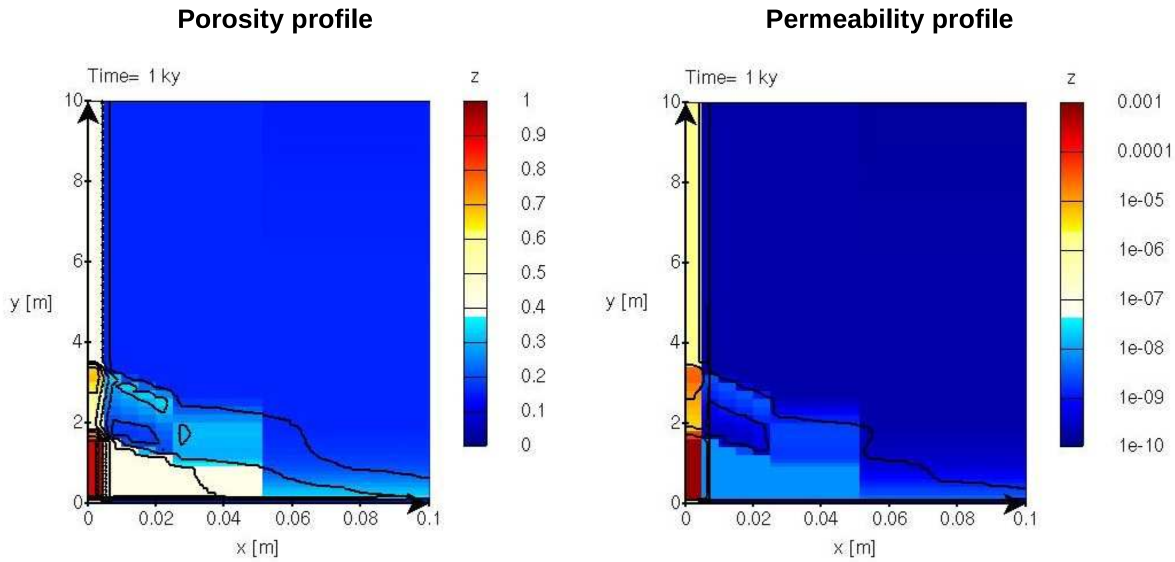

Figure 7. Distribution of porosity (left) and permeability (right, in m/s) after 1000 years of interactions between the caprock and dissolved CO_2. The discrete half-fracture is located at the left side of the domain (x < 5 mm).

The acceleration of the degradation is noticeable in the matrix close to the fracture: 1.5 m vertically at 1000 y (compared to a 0.4 m/10,000 y in the homogeneous *case 1c*) and in the fracture itself (4 m after 1,000 years). This is very dependant on the fracture properties: geometry (aperture), initial permeability, and initial carbonated filling.
This is potentially damaging for the sealing properties of the caprock, as opened fractures could create preferential pathways for SC-CO_2 due to lower local capillary entry pressure. As a consequence, the reactivity of the carbonated fracture sealing could be furthermore enhanced, and the reaction front in the fracture even faster.
This scenario is different from those already investigated in the literature focusing on the geochemical effects induced by the advancement of both a $CO_{2(aq)}$-rich aqueous phase and a free SC-CO_2 gas plume through a highly porous fractured caprock not filled in by secondary calcite (Gherardi et al., 2007). Under these conditions, the primary mineralogy of the caprock is predicted to be altered over the entire length of the fracture.

Generally speaking, the high reactivity of carbonated minerals, which can occur very soon in the life of the storage (as opposed to kinetically controlled clay mineral reactivity), raises a potential risk for the caprock integrity, particularly where these mineral phases are dominant such as in pre-existing fractures. If it appears that CO_2-saturated water, or SC-CO_2 can migrate through the caprock, and depending on the transport properties in the fractures, they could transport the acidic disturbance and potentially open critical pathways for CO_2.

5.3. Unsaturated caprock: geochemical interactions with SC-CO_2

These calculations correspond to the scenarios where the SC-CO2 plume make its way through the caprock either by overcoming the capillary entry pressure of by migration through an heterogeneity in the caprock (e.g., by mechanical and/or geochemical reactivation of a discrete fracture or a network of small cracks).

5.3.1. Homogeneous caprock and constant capillary properties

Case 3: In this section, we will consider the presence of CO_2 as a separate gas phase under supercritical thermodynamical conditions according to the considered temperature and pressure of 80°C and 150 bar, respectively. The simulations have been conducted using the reactive transport code TOUGHREACT. In the following, the term “gas phase” actually refers to SC-CO_2.
In this work, a shale thickness of 10 m is simulated and we focus on the geochemical impact of a possible capillary breakthrough of the gas phase in the caprock. Also, later in this work, we adjust the model of capillary pressure to alter the capillary entry pressure to allow the breakthrough capillary (see Appendix for a detailed explanation on the role of entry pressure on capillary trapping). It is important to note that this study does not deal with the estimation of the capillary entry pressure of the caprock overlying the Dogger in the Paris Basin geological context and we refer the reader to Chiquet et al. (2007) for a detailed study on this topic.

Relative permeability and capillary pressure model

In the framework of the Paris Basin, previous works have been performed to measure relative permeability and capillary pressure of the so-called Lavoux Limestone considered as a good analogue for the Dogger reservoir envisaged as a target for geological storage in

France (Lombard, 2008,. personal communication). In the following, we will assume similar trend for relative permeability and capillary pressure model although the cap rock and the reservoir pore structure may differ from one geological formation to another. Nevertheless, intrinsic permeability and porosity are chosen in agreement with the expected rock texture with values of 10^{-13}m² and 10^{-18}m² assigned to the reservoir and the caprock, respectively. André *et al*. (2007) have simulated the measured data using the following models:

$$K_{rl} = (S^*)^{0.5}\ (1-(1-(S^*)^{1/m})^m)^2 \tag{1}$$

with $S^*=(S_l-S_{lr})/(1-S_{lr})$; while the gas relative permeability data have been approximated by the following fourth degree polynomial function:

$$K_{rg} = 1.3978-3.7694S_l+12.709S_l^2-20.642S_l^3+10.309S_l^4 \tag{2}$$

with K_{rl} and K_{rg} the corresponding liquid and gaseous relative permeability phase, S_l the liquid phase saturation, $S_{lr} = 0.2$ the residual liquid phase saturation and $m = 0.6$ the van Genuchten exponent used in TOUGH2 (see Pruess, 1991). Capillary pressure is approximated also with a van Genuchten model described by:

$$P_{cap}=-P_o((S^{**})^{-1/m}-1)^{1-m} \tag{3}$$

with P_{cap} the capillary pressure, $S^{**} = (S_l-S_{lr})/(S_{ls}-S_{lr})$, and P_o a pressure coefficient which controls the magnitude of the capillary pressure model. In our simulations, we chose $S_{l\,s}= 1.05$, m=0.6 and P_o = 100 kPa to fit with the data of the Lavoux limestone and to allow the gas to enter the caprock (see Annexe). Intrinsic permeability values of 10^{-13}m² and 10^{-18}m² are assigned to the reservoir and the caprock, respectively.

Mesh and boundary conditions

The mesh geometry is taken similar to that of the study performed by Xu *et al.* (2005) to assess the integrity of a caprock composed with minerals of Texas Gulf Coast sediments. The geometry is 1D cartesian along the vertical direction with a 1 m² basal area, and 20 m long. The reservoir is represented as a unique cell, 10 m long, while the caprock is meshed with 17 cells progressively increasing in thickness from the reservoir-caprock interface to the top of the domain (from 0.05 to 1.00 m). The initial state of the system is a hydrostatic profile of pressure with uniform temperature at 80 C°. A constant pressure boundary was assigned to the top limit of the domain.

In order to assess the presence of CO_2 as a separate gas phase and compare this impact with the previous simulation, we kept the same initial mineralogical assemblage (Table 3) as well as a similar initial brine composition in the caprock (Table 2). On the other hand, the reservoir brine is acidified by adding a gas saturation value arbitrarily chosen to be 0.5. The CO_2 is assumed to remain in contact with the brine used as a reference (Table 2, column 1) composition before injection with an initial pressure of 150 bar.

Simulation Results

Figure 8 shows the simulated upward migration of the gas saturation front through the caprock. After ten years the CO_2 plume has penetrated one meter into the caprock, at 1000 years it reaches 5 m, and at 10 000 years gas has entered about 8 m into the caprock. This upward migration is controlled by both the capillary entry pressure and the intrinsic permeability of the caprock. The main process of migration is due to buoyancy effect. Indeed, at 80°C and 150 bar, gas and brine density are equal to 430 and 1020 kg/m^3, respectively. The pH calculated for the reservoir system equals 4.7 (Figure 9), in good agreement with the homologous single phase simulation scenario previously presented (*Case 1a*). The gas front is preceded by the dissolution of the gas phase in the brine which acidifies the system. As an indication, the results of the single-phase and 2-phase simulations are compared in Figure 9.

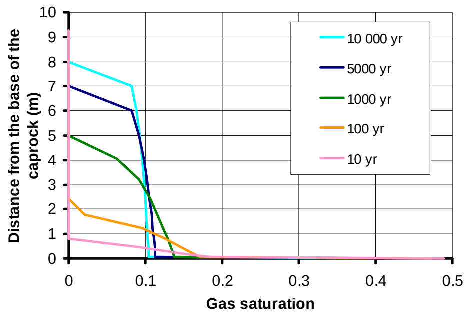

Figure 8. Gas saturation profiles in the caprock at 10, 100, 1000 and 10 000 years

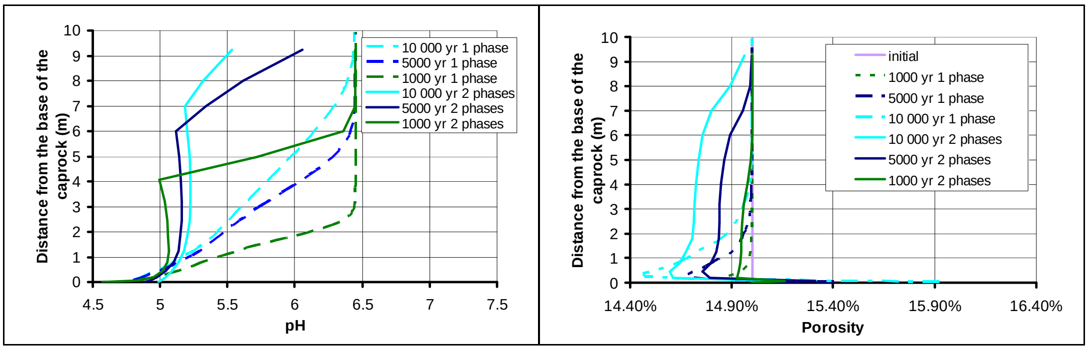

Figure 9. pH and porosity profiles at 1000, 5000 and 10 000 years. Comparison with the single phase case

After 10 000 years, the simulations predict a small porosity change similar, in amplitude, to that observed for the single phase case (*case 1a*) but with a larger extent (Figure 9). This porosity variation is controlled by the mineral dissolution and precipitation processes which are comparable to that of the single phase scenario. Therefore, considering SC-CO_2 in the simulation scenario is crucial for the estimate of the capillary trapping in the caprock which is controlled by the capillary entry pressure and the thickness of the reservoir. On the other hand, if SC-CO_2 penetrates in the caprock, the induced geochemical alteration of the shale formation does not differ much from the purely diffusive case prediction, but the affected region will occupy a larger extent controlled by the gas plume geometry.

Other authors in the literature reached the same conclusions with slightly different reactive pathways and consequences on porosity, again due to the presence of plagioclase minerals and the precipitation of minerals such as dawsonite (Xu et al., 2005). In contrast, in some cases (Johnson et al., 2004; Gherardi et al., 2007), and depending on variable conditions of gas saturation and initial mineralogy, major variations in porosity have been predicted in the caprock in association with relevant precipitation of other carbonate minerals such as magnesite and calcite.

6. DISCUSSION

The results of the modeling show that the injection of CO_2 can potentially have a significant effect on the caprock by changing the mineralogy and changing the porosity due to the dissolution and precipitation of minerals. Although these changes will in turn induced changes in the transport properties of the caprock, the impact is limited to a zone ranging from several decimeters to several meters into the caprock close to the interface with the reservoir depending on whether the SC-CO_2 plume enters into the caprock and/or if fractures are present at this location (Table 6).

	pH		Porosity	
	Minimal value	Impact distance into caprock	Absolute change (- clogging, + opening)	Impact distance into caprock
Saturated homogeneous caprock				
Case 1a (with pH perturbation)	4,8	8 m	- 0.2% + 1.8 %	0.5 - 1.5 m 0.1 - 0.2 m
Case 1a (without pH perturbation)	6,2	7 m	+ 2.2 %	0.1 - 0.2 m
Case 1b (pH 4.6)	4,6	8 m	- 7% - 1%	0.01 m 2.5 m
Case 1b (pH 3.4)	3,4	8 m	+ 70% + 40%	0.05 m 0.5 m
Case 1c (diffusion-advection)	3,4	0.5 m	+ 27% + 18%	0.35 m 0.5 m
Saturated fractured caprock				
Case 2 **(1000 y)**			+ 25%	1.5 m (vertical) 0.05 m (horizontal)
Unsaturated caprock				
Case 3	4,8	10+ m	- 0.5% + 1 %	0.5 - 6 m 0.1 - 0.2 m

Table 6. Overview of minimal pH value and porosity changes with the perturbation distance according to the different scenarios (after 10 000 years or otherwise mentioned in the table).

Heterogeneities in caprock composition and properties

The presence of fractures with a different composition and set of transport properties is crucial for the extension of the perturbation. The results obtained with the fracture in the *case 2* show the potential role of other types of heterogeneity, such as the intrinsic heterogeneity of mineralogical composition or the presence of a network of small cracks in the caprock. The geochemical behavior in these systems is intricately coupled with the behavior of the CO_2 plume, through the heterogeneity of capillary properties as demonstrated for instance by Saadatpoor et al. (2009).

The difference between the reactivity of carbonates and clay minerals is the key to the evolution of the system: short term and short distance for carbonates, long term and long distance for the clay minerals (see *case 1b* and *case 3*). To this regard, one cannot exclude the role of clay transformations such as the illitisation of smectite or illite/smectite interstratified minerals, which is observed in experiments (Crédoz et al., 2010) and potentially represents a further change of properties for the caprock (porosity, permeability, wettability).

Conditions for gas entry into the caprock

In a series of scoping hydraulic/geomechanical calculations (Rohmer and Seyedi, 2009), the maximal capillary pressure calculated for an industrial-scale injection of CO_2 into a deep saline aquifer (1 Mt CO_2/yr) is less than 2 bar at the reservoir-caprock interface, far below the capillary entry pressure of most caprocks (see results from WP2, Carles et al. 2009; and Talandier et al. 2006). These results imply that in the conditions of the calculations, the SC-CO_2 plume would not enter into the caprock in the case of a caprock with homogeneous properties. This conclusion has to be reassessed in the case where heterogeneities in the caprock mineral composition could affect the local properties of the rock (such as the capillary curve or relative permeabilities). Also, for injection periods of 10 to 100 years, induced plume entry can be triggered by chemical alteration modifying the pore sizes and structure in the caprock: this scenario was investigated during the project but the model is still under development and shows numerical instability. The pH changes due to the presence of CO_2 can also potentially modify the mineral wettability, although this is still a controversial matter (see e.g. Chiquet et al., 2007; Shah et al. 2008; Fleury et al, *this issue*).

During injection, the total overpressure is significant only at the vertical of the injection point (ΔP = 35 bar in Rohmer and Seyedi, 2009) after 10 years of injection and drops to a few bar after the injection stops. These results tend to discard any direct mechanical effect such as fracturing in the caprock during and after the injection phase. Nevertheless, coupled mechanical and chemical processes, such as evidenced here, are maximal in the case of long periods of injection (10 to 100 years) because this would be the typical timescale for carbonate chemical alteration. This phase may turn out to be critical especially with respect to the alteration of the sealing properties of the caprock (Bemer and Lombard, 2009).

Consequences of gas entry into the caprock

The results of the calculations with the complete mineralogical and geochemical system predict no significant differences between the case with or without gas entry into the caprock in terms of amplitude of the porosity variations. However, differences are observed on the extent of the impacted zone within the caprock: several meters in the "gas entry" cases whereas it is limited to the first decimeters near the reservoir-caprock interface in the cases without gas entry.

7. CONCLUSION

The results of the modeling of safety scenarios show that in the normal reference case (homogeneous rock, diffusion of dissolved CO_2 only) the impact of the reactivity with CO_2-rich fluids with the carbonate minerals potentially induces significant changes of porosity. Nevertheless, this reactivity is limited to the first decimeters of the caprock close to the interface with the reservoir in 10 000 years and does not lead to any leak from the storage system.

Calculations in "degraded" scenarios show that the migration of the perturbation due to SC-CO_2 can extend to several meters within the same period of 10 000 years. These scenarios involve either an alteration of the petrophysical properties of the rock due to the reactivity with CO_2-rich solutions (potentially enhancing small existing heterogeneities) or the reactivation of small cracks or fractures (especially if they are filled with calcite). In both cases, preferential pathways are created for the migration of CO_2 and positive feedback is involved, i.e. more migration leads to more reactivity and more alteration of the transport properties. In these scenarios, any convective component occurring as a result of the alteration will renew and feed the acid perturbation at critical locations (e.g. richer in carbonates minerals), and can in turn extend the migration distance of CO_2. One of the key points for the safety assessment calculations remains the role of these heterogeneities on the behavior of the storage system. We observe in this work the great influence of structural heterogeneities. The quantitative assessment of such an impact on the global safety remains an important challenge.

To complete a safety assessment for a specific site, a set of conservative (penalizing) parameters should be adopted for adverse scenarios (such as in *case 1b*) to evaluate the quantity of CO_2 release from the storage system and the probability of occurrence of these scenarios should be evaluated from data available from this site (Bildstein *et al*. 2009). The challenge for the future will be to structure and apply the safety assessment methodology with an operational finality, in order to support the transition step to carbon geological storage projects at the industrial scale.

8. ACKNOWLEDGEMENTS

The authors acknowledge funding from the ANR (the French National Science Foundation) in the framework of the “Géocarbone” projects (Injectivité, Carbonatation, PICOREF, CRISCO2) and fruitful discussion with the other partners in these projects. This project also benefited greatly from the scientific exchanges taking place in the working group “Modeling at the site scale” animated by E. Brosse (IFP).

9. APPENDIX: ROLE OF ENTRY PRESSURE ON CAPILLARY TRAPPING

Figure 10 shows the pressure fields of water and carbon dioxide in a geological storage in aquifer located at a depth *H* underneath the surface. Once injected, CO_2 occupies the reservoir pore space available initially filled with water. Due to gravity effects, the storage area, containing both CO_2 and residual water, is located at the top of the aquifer and has a thickness *h*. Point **A** is located at the interface between reservoir and caprock and is part of the caprock domain. Point **A’** is also located at the interface between reservoir and caprock but belongs to the reservoir domain. Point **B** is located at the gas-water contact. At this interface the capillary equilibrium is reached and the capillary pressure is zero. In other words in **B**:

$$P_{B,CO2}=P_{B,H2O}$$

In **A**, the water pressure is equal to the water column in the caprock:

$$P_{A,H2O} = \rho_{H2O}\, g\, H$$

In **A'**, the CO_2 pressure $P_{A',CO2}$ is equal to:

$$P_{A',CO2}=P_{A,H2O}+P_{cap}$$

with P_{cap}, the capillary pressure defined as the difference between gas pressure and water pressure.

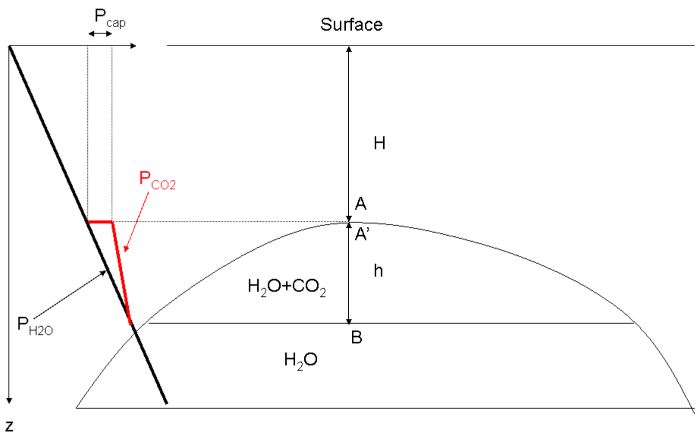

Figure 10 : CO_2 and H_2O pressure evolution with depth in aquifer storage

In the context of geological storage, we define the capillary entry pressure as a capillary pressure threshold representing the resistance of porous network saturated with water to the penetration of carbon dioxide. The capillary entry pressure P_{ce} is intrinsic to the nature of the pore network constituting the clay caprock. According to the Laplace law, it can be expressed as:

$$P_{ce} \sim 2\sigma \cos(\phi)/R,$$

with σ the inter-facial tension between the liquid and gas, ϕ the angle reflecting the ability of the liquid to spread over a surface by wettability, and R the radius of the largest pores (Chiquet et al 2007).

The capillary entry pressure is the value of capillary pressure for a zero gas saturation (Figure 11). The van Genuchten model used in the code Toughreact adjusts the capillary entry pressure using the liquid parameter saturation S_{ls}. For $S_{ls} > 1$, the model of capillary pressure becomes non zero for $S_g = 0$ (Figure 11).

If the capillary pressure at the caprock-reservoir interface exceeds the capillary entry pressure ($P_{cap\text{-}interface} > P_{ce}$), then the CO_2 can penetrate the caprock.

The capillary pressure in the reservoir-caprock interface $P_{cap\text{-}interface}$ is expressed as:

$$P_{cap\text{-}interface} = P_{A',CO2} - P_{A,H2O}$$

Assuming no change with depth in both CO_2 and H_2O densities, we can write:

$$P_{A',CO2} = P_B - \rho_{CO2} g h$$

$$P_{A,H2O} = \rho_{H2O} g H$$

On the other hand, considering that:

$$P_B = \rho_{H2O}\, g\, (H+h)$$

We finally obtain:

$$P_{cap\text{-}interface} = (\rho_{H2O}\text{-}\rho_{C2O})\, g\, h$$

This corresponds to the buoyancy effect induced by density difference between liquid and gas.

Thus, for the gas phase to penetrate the caprock, we must verify that:

$$P_{ce} < (\rho_{CO2}\text{-}\rho_{H2O})\, g\, h$$

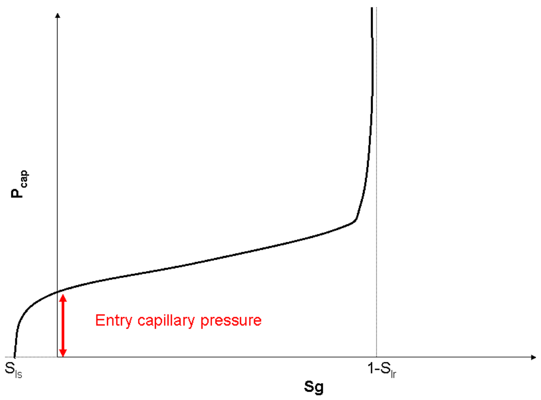

Figure 11 : Representation of the entry capillary pressure using the van Genuchten model as described in the code TOUGHREACT

In our system, we assume a 10 m thickness for the reservoir. At 150 bar and 80°C, the density of CO_2 is about 430 kg/m^3, while the density of water is 1018 kg/m^3, which leads for a 10 m thick reservoir to a value of $P_{cap\text{-}interface}$ of 57 kPa (0.57 bar). Using a value of P_o = 100 kPa in Eq(3) yields a P_{ce} of 54 kPa slightly below $P_{cap\text{-}interface}$ and then allowing CO_2 to penetrate the caprock.

10. REFERENCES

André L., Audigane. P., Azaroual. M., Menjoz. A. (2007) Numerical modelling of fluid-rock interactions at the supercritical CO2-liquid interface during carbon dioxide injection into a carbonate reservoir, the Dogger Aquifer (Paris basin, France), *Energy Conversion and Management* **48**, 1782-1797

Azaroual M., Fouillac C., Matray J.M. (1997) Solubility of silica polymorphs in electrolyte solutions, II. Activity of aqueous silica and solid silica polymorphs in deep solutions from the sedimentary Paris Basin, *Chemical Geology* **140**, 167-179.

Bemer E., Lombard J.M. (2009) From injectivity to integrity studies of CO2 geological storage: impact of low permeability levels on the experimental investigation of chemical alteration effects on rock petrophysical and geomechanical properties, *Oil Gas Sci. Tech.*, this issue.

Berne Ph., P. Bachaud, M. Fleury (2009) Diffusion properties of carbonated caprocks from the Paris Basin, *Oil Gas Sci. Tech.*, this issue.

Bildstein O., Jullien M., Crédoz A., Garnier J. (2009) Integrated modeling and experimental approach for caprock integrity, risk analysis, and long term safety assessment, Proceedings of the GHGT-9 conference, Washington DC, *Energy Procedia* **1**, 3237-3244.

Carles P., P. Bachaud, E. Lasseur, P. Berne, P. Bretonnier (2009) Confining properties of carbonaceous Dogger caprocks (Parisian Basin) for CO_2 storage purposes, *Oil Gas Sci. Tech.*, this issue.

Chiquet P., Broseta D., Thibeau S (2007) Wettability alteration of caprock minerals by carbon dioxide, *Geofluids* **7**, 112–122.

Crédoz A., Bildstein O., Jullien M., Géniaut G., Lillo M., Pétronin J.C., Pozo C., Raynal J., Trotignon L., Pokrovsky O. (2009) Experimental and modeling study of geochemical reactivity between clay minerals and CO_2 in geological conditions, proceedings of GHGT-9 conference, Washington DC., *Energy Procedia* **1**, 3445-3452.

Crédoz A., Bildstein O., Jullien M., Raynal J., Trotignon L., Pokrovsky O. (2010) Mixed-layer illite-smectite reactivity in co2-bearing solution: implications for clayey caprock stability in co2 geological storage, *Appl. Clay Sci., submitted*

Duan Z., Sun R. (2003) An improved model calculating CO2 solubility in pure water and aqueous NaCl solutions from 273 to 533 K and from 0 to 2000 bar, *Chemical Geology* **193**, 257– 271

Fleury M., Berne P., Bachaud P. (2009) Diffusion of dissolved CO2 in caprock, Proceedings of the GHGT-9 conference, Washington DC, *Energy Procedia* **1**, 2009.

Fleury M., Kervévan, C., Bildstein, O., Lagneau, T. Pichery, S. Fillacier, M. Lescanne (2009). Géocarbone-Intégrité program, *Oil & Gas Sci. Tech.*, this issue.

Gauss I., Azaroual M., Czernichowski-Lauriol I. (2005) Reactive transport modelling of the impact of CO2 injection on the clayey cap rock at Sleipner (North Sea), *Chemical Geology* **217**, 319– 337

Gauss I., Audigane P, André L., Lions J., Jacquemet N., Durst P., Czernichowski-Lauriol I., Azaroual M. (2008) Geochemical and solute transport modelling for CO2 storage, what to expect from it? *Int. J. Greenhouse Gas Cont.* **2**, 605-625

Gherardi F., Xu T., Pruess K. (2007) Numerical modeling of self-limiting and self-enhancing caprock alteration induced by CO_2 storage in a depleted gas reservoir, *Chemical Geology* **244**, 103–129

Hildenbrand A., Kroos B.M. (2003) CO_2 migration processes in argillaceous rocks: pressure-driven volume flow and diffusion. *Journal of Geochemical Exploration* **78-79**, 169–172.

Hubert G. (2009), Réactivité expérimentale au CO2 de roches d'une couverture argileuse et d'un réservoir carbonaté du bassin de Paris. Experimental reactivity with CO2 of clayey caprock and carbonate reservoir of the Paris basin. PhD Thesis, INPL, Nancy, France, 370 p.

IPCC (2005) IPCC Special Report on Carbon Dioxide Capture and Storage. Prepared by Working Group III of the Intergovernmental Panel on Climate Change [Metz, B., O. Davidson, H. C. de Coninck, M. Loos, and L. A. Meyer (eds.)]. Cambridge University Press, Cambridge, United Kingdom and New York, NY, USA, 442 pp.

IPCC (2007) Climate Change 2007: Synthesis Report. Contribution of Working Groups I, II and III to the Fourth Assessment. Report of the Intergovernmental Panel on Climate Change [Core Writing Team, Pachauri, R.K and Reisinger, A. (eds.)]. IPCC, Geneva, Switzerland, 104 pp.

Johnson J.W., Nitao, J.J., Knauss, K.G. (2004) Reactive transport modeling of CO2 storage in saline aquifers to elucidate fundamental processes, trapping mechanisms, and sequestration partitioning. In: Baines, S.J., Worden, R.H. (Eds.), Geologic Storage of Carbon Dioxide. *Geol. Soc. London Spec. Pub*. **233**, 107–128.

Johnson J.W., Nitao, J.J., Morris, J.P. (2005) Reactive transport modeling of cap rock integrity during natural and engineered CO2 storage. In: Thomas, D.C., Benson, S.M. (Eds.), *Carbon Dioxide Capture for Storage in Deep Geologic Formations*, vol. 2, 787–813.

Kohler E., Parra T. (2007) Clayey cap-rock behavior in H2O-CO2 media at low pressure and temperature conditions : an experimental approach, 44th Annual Meeting of the Clay Minerals Society, June 2-7, Santa Fe, USA

Le Gallo Y., Trenty L., Lagneau V., Audigane P., Bildstein O., Mugler C. & E., Mouche (2007) Recent development for long term modeling of CO2 storage. *In* First French-German Symposium on Geological Storage of CO_2 (Ed A. C. Geotechnologien), GfZ Potsdam.

Mathias S.A., Hardisty P.E., Trudell M.R., Zimmerman R.W. (2009) Screening and selection of sites for CO2 sequestration based on pressure buildup, *Int. J. Greenhouse Gas Cont*. **3**(5), 577-585

Mavko G., Nur A. (1997) The effect of a percolation threshold in the Koseny-Carman relation, *Geophysics* **62**(5), 1480-1482.

Palandri J., Kharaka Y.K (2004). A compilation of rate parameters of water-mineral interaction kinetics for application to geochemical modelling. US Geological Survey Open File Report 2004-1068

Parkhurst D.L., Appelo C.A.J., (1999) - User's guide to PHREEQC (Version 2)--A computer program for speciation, batch-reaction, one-dimensional transport, and inverse geochemical calculations: U.S. Geological Survey Water-Resources Investigations Report 99-4259, 312 p.

Parkhurst D.L., Kipp K.L., Engesgaard P., Charlton S.R. (2004) – PHAST, a program for simulating ground-water flow, solute transport, and multicomponent geochemical reactions. U.S. Geological Survey Techniques and Methods 6-A8, 154 p.

Pruess, K., 1991, TOUGH2 – a general-purpose numerical simulator for multiphase fluid and heat flow: Lawrence Berkeley Laboratory Report LBL-29400, Berkeley, California

Rohmer J., D. Seyedi (2009) Addressing caprock failure tendency in deep saline aquifers through large scale hydromechanical analysis: Application to the CO2 geological storage in the Paris basin case, *Oil Gas Sci. Tech*, this issue.

Saadatpoor E., Bryant S.L., Sepehrnoori K. (2009) Effect of capillary heterogeneity on buoyant plumes: A new local trapping mechanism, proceedings of GHGT-9 conference, Washington DC., *Energy Procedia* **1**, 3299-3306.

ShahV., Broseta D., Mouronval G. (2008) Capillary alteration of caprocks by acid gases, SPE 113353-PP, Improved Oil Recovery Symposium, Tulsa, OK, USA, 19-23 April 2008.

Steefel C.I. (2001) CRUNCH: Software for modeling multicomponent, multidimensional reactive transport. User's Guide, UCRL-MA-143182. Livermore, California.

Talandier J., Mayer G., Croisé J. (2006) Simulations of the hydrogen migration out of Intermediate-level radioactive waste disposal drifts using tough2, Proceedings TOUGH Symposium, Lawrence Berkeley National Laboratory, Berkeley, California

van der Lee J., L. De Windt, V. Lagneau, and P. Goblet (2003) « Module-oriented modeling of reactive transport with HYTEC », *Computers and Geosciences* **29**, 265-275

Wolery T.J., (1992). EQ3NR, a Computer Program for Geochemical Aqueous Speciation-Solubility Calculations: Theoretical Manual, Users Guide, and Related Documentation (Version 7.0). Lawrence Livermore National Lab. Report UCRL-MA-110662 PT IV.

Xu T., Pruess, K. (2001), Modeling multiphase non-isothermal fluid flow and reactive geochemical transport in variably saturated fractured rocks: 1. Methodology: *American Journal of Science* **301**, 16-33.

Xu T., Apps, J., Pruess, K. (2005), Mineral sequestration of a sandstone-shale system: *Chemical Geology* **217**(3-4), 295-318.